TURBULENT BOUNDARY LAYER SHEAR STRESS PULSES IN ADVERSE PRESSURE GRADIENT

V. A. Sandborn
Department of Civil Engineering
Colorado State University
Fort Collins, Colorado 80525, USA

ABSTRACT

Experimental evaluation of the time dependent surface shear stress or heat transfer in adverse pressure gradient turbulent boundary layers was studied. Surface shear stress pulses as great as three to eight times the **mean** values were indicated in the adverse pressure gradient flows. The minimum time dependent surface shear stress varied from 0.2 to 0.4 times the mean shear as Reynolds number increased in the adverse pressure gradient flows. Although it was not possible to evaluate the surface shear stress in the separation region, laser velocimeter measurements indicate independent positive and negative velocity pulses are present in the wall region.

The statistical characteristic times between the largest shear stress pulses was correlated using the mean skin friction coefficient and a function of the velocity profile form factor and Reynolds number for a wide range of flow conditions.

INTRODUCTION

Experimental evaluation of the time dependent heat transfer and/or surface shear stress indicate large amplitude pulses are always present, Sandborn (1998). The large pulses in surface shear stress are the major factor in the movement of sediment and snow, as well as local forces on structures such as roofs. While considerable data has been reported for the zero pressure gradient flows, only limited evaluation related to the pulses have been reported for pressure gradient flows.

Experimental study of the time dependent surface shear stress in zero pressure gradient boundary layers was reported by Sandborn (1998). It was demonstrated that a time dependent impulse-mean flow solution could predict the **mean** surface shear stress for the lowest Reynolds numbers (R_θ <500). For the higher Reynolds numbers, typical of aerodynamic flows, the initial large shear pulses were not as dominate a factor in the mean surface shear stress.

Analytical evaluation using "Large Eddy Simulation" indicate the occurrence of streamwise vortices within the viscous sublayer, Robinson (1991). These calculations are limited to the very low Reynolds numbers, and have not been able to predict the surface shear stress, Jimenez (1998). It is not obvious that the vortices within the sublayer could produce impulses equivalent to 0.8 times the freestream velocity.

The present experimental study was directed toward the evaluation of the time dependent surface shear stress in pressure gradient flows. Both highly curved surfaces leading to turbulent boundary layer separation and pressure rises along a flat surface were used in the study.

SURFACE SHEAR STRESS PULSES

Surface shear stress pulses are found in all turbulent surface shear flows. They appear to persist into the separation region. The magnitude of the pulses are large throughout the adverse pressure gradient region. The insert on figure 1 shows a typical surface hot wire voltage-time traces taken in an adverse pressure gradient flow. The measured pressure rise for the flow can be seen on figure 2b). The trace was taken along the flat, top surface of a 61x61cm tunnel, which had a false floor to produce the pressure gradient, figure 2, The range of flow conditions for the present study are shown on figure 2.

The expanded time trace, figure 1, demonstrates both the magnitude and time associated with a typical large pulse. (The time dependent surface shear stress evaluation is limited to approximately two place accuracy.) The maximum pulse magnitudes were found to vary widely from 3 to 8 times the mean surface shear stress for a given flow in the adverse pressure gradient, compared to values of approximately 3 for the zero pressure gradient flow. Both the magnitude and time of occurrence of the pulses appear more random for the

adverse pressure gradient flows. A non-dimensional time scale T^+ ($U_\tau^2 t/\upsilon$) is also noted on figure 1. Rise time values of T^+= 8 to 10 were found for both the zero and adverse pressure gradient flows. The non-dimensional rise time did not appear sensitive to the flow conditions. An approximate analysis of the interaction of a streamwise vortex with a surface, Orlandi and Jimenez (1994), indicated that the spanwise surface shear increased by a factor of two in a time of T^+=5.

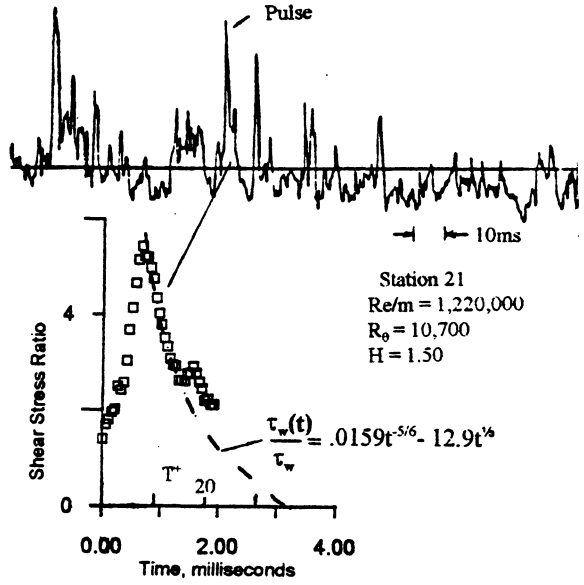

Figure 1.Time history of typical surface shear stress pulses.

The present hot wire sensors were purposely limited in length ($\ell/d \leq 100$) in order to obtain approximate point measurements. For these small ℓ/d the sensors are much hotter in the center, and thus more sensitive, over very short distances, to the surface shear stress. The short sensors were less sensitive to the direction of the surface shear stress during a pulse than that of a longer sensor. The probability that the pulses were not perpendicular to the sensors did not appear to alter the measured rise times.

As demonstrated for the zero pressure gradient case, Sandborn (1998), the initial pulses appear to correspond to velocity pulses of the order of 0.8 times the freestream velocity, U_e. The pulses in the adverse pressure flows are thought to correspond to velocities of the order of $0.8U_e$. Experimentally the pulse appears to approximate an impulsively started flow coupled with a residual viscous boundary layer. Similarity solutions for impulsively started flows, Watson (1955), indicate that the surface shear stress should decay as

$$\tau_w(t) = \frac{\rho U_i \sqrt{\nu}}{\sqrt{t}}[\phi_o(0) + AF'(x)\phi_1(0)t^{\alpha+1} + \mathcal{O}(t^{2\alpha+2}) + \ldots] \quad (1)$$

for an impulse velocity of the form $U_i(x,t) = AF(x)t^\alpha$. For the zero pressure gradient flow, [F'(x)=0], Sandborn (1998), the particular case α = -.25 was used to satisfy the requirement $(\partial^2 U/\partial y^2)_{y=0}$=0. For adverse pressure gradient flow

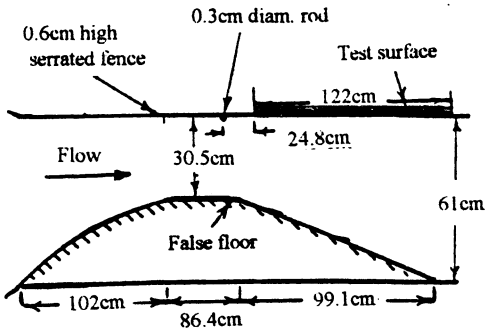

a) Tunnel configuration

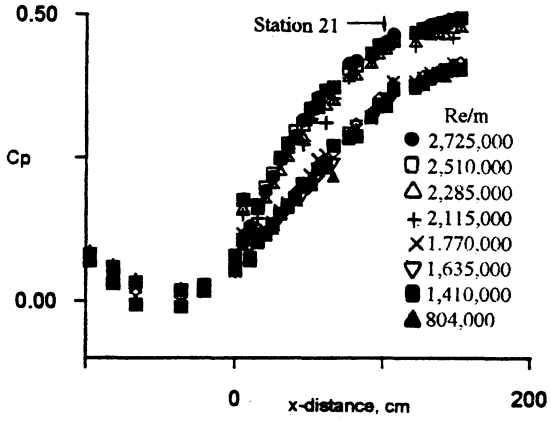

b) Pressure distribution

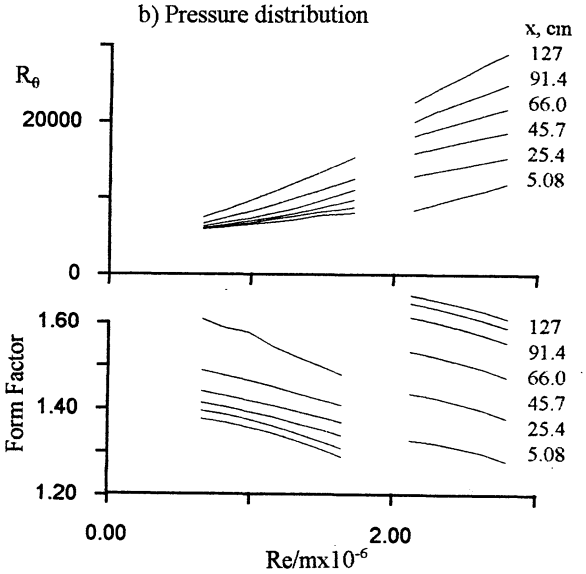

c) Reynolds number and form factor

Figure 2. Flow Properties in the 61x61 cm tunnel.

$(\partial^2 U/\partial y^2)_{y=0}<0$, so $\alpha<-.25$ is required. [The solution, Watson (1955), was valid only for $\alpha \geq -.5$. The impulse velocity is ill defined at t=0.] Using a value, $\alpha = -1/3$ the surface shear stress decays with time as

$$\tau_w(t) = Bt^{15/6} + Ct^{1/3} + Dt + \ldots \quad (2)$$

For adverse pressure gradients the factor C [$= \rho\sqrt{\nu}AF'(x)$] is negative (i.e. F'(x) is negative). The factor D contains terms related to F" and $(F')^2$, so its sign and magnitude will depend on the particular flow. An estimate of the pulse decay, neglecting the higher order terms ($D \approx 0$), is shown as the dashed curve on figure 1. The decay predicted by equation (2), neglecting the D term, appears to be realistic for the present flow. If the decay occurs as noted on figure 1, the surface shear stress would reach zero 3.2 milliseconds after the start of the pulse. A more realistic model would, however, require the impulse decay be altered once the velocity, $U_i \propto t^{-\alpha}$, decreases to the convective velocity of the pulses, Sandborn (1998).

The occurrence of secondary pulses during the decay, such as seen on figure 1, appeared quite often. Although an overlap pulse may occur due to the finite length of the sensor, the secondary pulses are also seen with vertical wire sensors. These secondary pulses may be an integral part of the vortex-surface interaction process.

The minimum values of the time dependent surface shear stress varied from 0.4 times the mean shear at the high Reynolds numbers to 0.2 at the lower Reynolds number in the 61x61 cm tunnel. As noted above the simple decay of the pulse would reach zero surface shear very quickly. The model proposed by Sandborn (1998) requires the decay be checked by the occurrence of a "steady-state-residual" viscous layer due to the convective velocity of the pulse along the surface. The streamwise vortices may also contribute to surface shear stress.

Flow separation region.- The surface hot wire sensors can not follow the separation process once flow reversal occurs. The sensors do, however, indicate the large positive pulses of surface shear stress persist well into the separation region. As the flow proceeds into the separation region the individual events may develop small, local zero-surface-shear-stress regions. These local "separations" would appear to increase in size and number with distance until they are perceived as back flow by the laser velocimeter.

The simple build up of reverse flow within individual events appears realistic for the "flat-plate" type flows.. Unfortunately, most practical adverse pressure gradient turbulent boundary layer flows include curvature of the surface. A small 8.9x16.5cm, 2-dimensional diffuser tunnel was employed to study the separation region on a curved surface. A well developed separation region was obtained. Figure 3 shows a set of velocity probability distributions measured near the surface (y=1.3mm), obtained with a laser velocimeter, for a number of different locations within the separation region. These velocity probability results together with flow visualization indicated a global aspect of separation rather than the local pulse-decay concept.

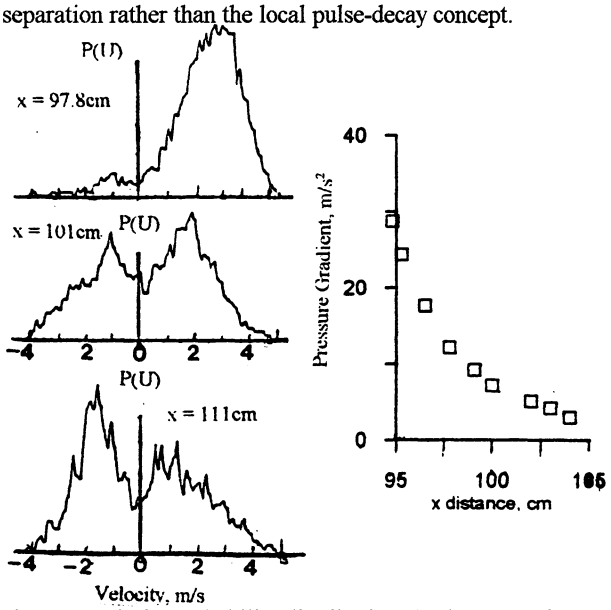

Figure 3. Velocity Probability distributions in the separation region.

Once the backflow was established the reverse flow appeared as pulses of velocity coming from some distance downstream. The development of **bimodal** probability distributions demonstrate that the forward and reverse pulses of flow are independent of one another. When the forward and reverse flows meet small vertical motions occur. Observations of the separation regions in river flows are found to be extra turbid, due to the small "tornados" stirring the sediment.

Pulse timing.-A characteristic statistical time between pulses was determined by counting the number of pulses during a given time period. For the zero pressure gradient flow and the flow in the small 8.9x16.5cm tunnel an amplitude discrimination, counting technique using an EPUT counter was employed, Sandborn (1998). The counting technique allowed time periods of the order of 100 seconds to be used for the averaging. The statistical measurements were repeatable to only two significant figures. Evaluation of the non-dimensional times between pulses for the zero pressure gradient flows indicated they corresponded to the coherent event times (bursting frequencies) obtained from flow visualization, Kline, et al. (1967). Thus, the large surface shear stress pulses may be the footprint of the coherent events. It was further demonstrated that the non-dimensional times correlated with the skin friction coefficient for the zero pressure gradient flows, figure 4. As shown on figure 4, the adverse pressure gradient flows require at least another parameter to correlate the non-

Dimensional time and the skinfriction.

Figure 5 shows typical variations of the non-dimensional time between pulses as a function of inlet Reynolds number

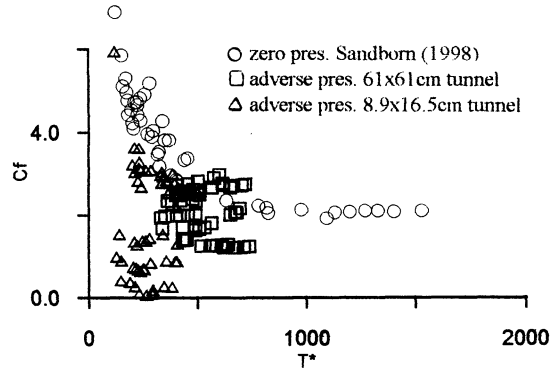

Figure 4. Skin friction variation with the pulse time.

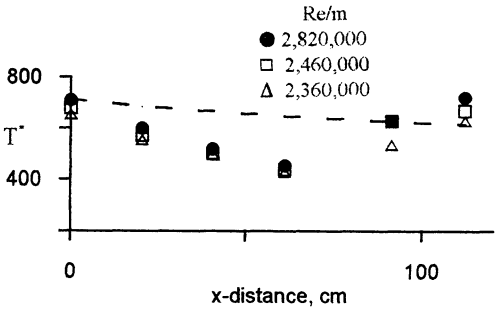

Figure 5. Variation of the pulse time along the test wall.

Along the test wall of the 61x61 cm tunnel. The dashed line indicate the variation of T^* (for Re/m= 2,820,000) if the time between pulses is held constant and only the freestream velocity decreases. The **non-dimensional** time increased with Reynolds number at all locations along the test section.

Schraub and Kline (1965) attempted to correlate the event times using a non-dimensional pressure gradient parameter K [$= -\nu/U_\infty^3(1/\rho)(dp/dx)$]. This parameter would appear to be limited to local flow conditions, and not representive of the history of the boundary layer. For pressure gradient flows Ludwieg and Tillmann (1949) demonstrated that the turbulent boundary layer history could be accounted for by employing the momentum thickness Reynolds number, R_Θ, and the form factor, H. Thus, a function, $f(H,R_\Theta)$ was sought to correlate the data shown on figure 4. The function

$$f(H,R_\Theta) = [2.67 - H + \frac{2.45x10^5}{R_\Theta} \exp- \frac{(\ln R_\Theta - 14)^2}{7.39}]$$

$$[1.94x10^{-4}+8.96x10^{-3}H^{-4}] \qquad (3)$$

was employed to correlate the data. The first term in the brackets of equation (3) is a separation criterion, Sandborn (1979). This bracket goes to zero at the point of separation where the mean-surface-shear-stress is zero, thus both positive and negative value of c_f will result in positive values of T^*. Figure 6 is a plot of the present measurements and the zero

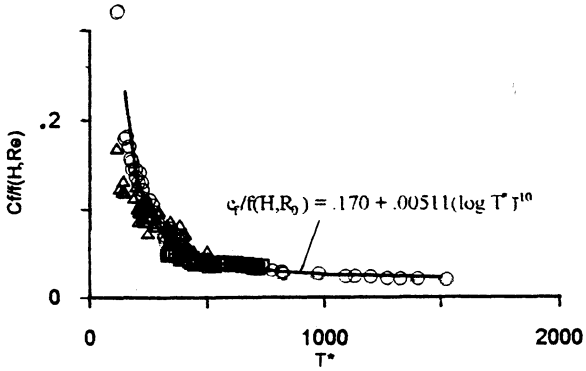

Figure 6. Correlation of the non-dimensional pulse times.

pressure data for $c_f/f(H,R_\Theta)$ versus T^*. An approximate curve fit of the data is noted on figure 6.

Figure 7 is a plot of previous reported event times (burst frequency) for pressure gradient flows compared with the

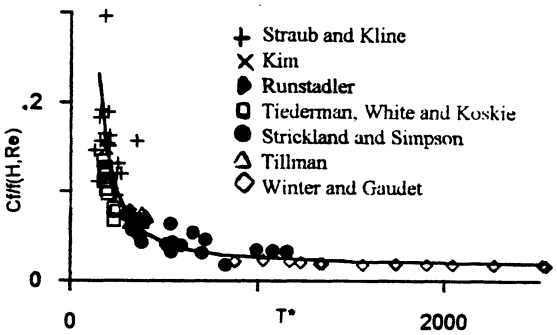

Figure 7. Comparison of time scales for previously reported burst times.

equation noted on figure 6. The data of Straub and Kline (1965) contain three points that were identified as relaminarization flows. Two of the three relaminarization flow times agree with the present correlation, while the third flow (T^*= 350) suggest the conditions are more laminar than turbulent. The data point of Strickland and Simpson (1977) at T^*= 1155 is for a flow where c_f is negative. The data of Winter and Gaudet (1970) contain direct measurements of c_f, however, the values of T^* were not measured. For the Winter-Gaudet data the values of T^* were calculated from the relation for zero pressure gradient flow given by Sandborn (1998)

$$T^* = 27 + 6.73R_\theta^{0.483} \qquad (4)$$

The measurements of Winter and Gaudet indicate that the present correlation can be used at the extremely high Reynolds numbers (R_θ>200,000).

Event speed.-For the zero pressure gradient flows the convection velocity of the pulse events was found to be approximately 0.6 times the freestream velocity (independent of Reynolds number), Sandborn (1998). Measurements of convective velocity in the adverse pressure gradient were limited due to the lack of persistence of the pulses. It was difficult to identify the same pulse for distances greater than 5 to 10 millimeters. Figure 8a) shows surface-hot-wire voltage traces for two sensors separated by a distance of 0.53mm

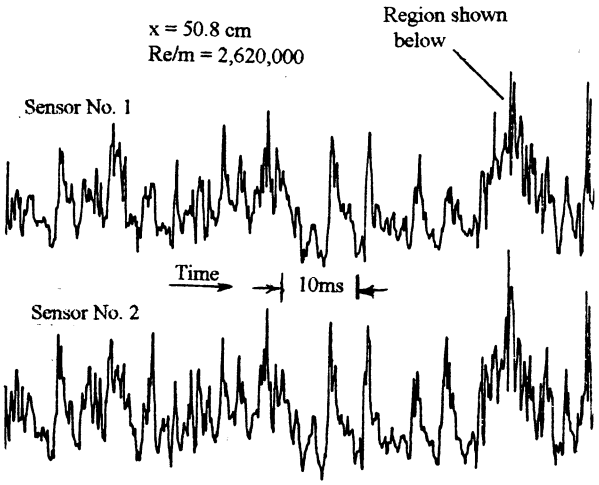

a) Voltage traces

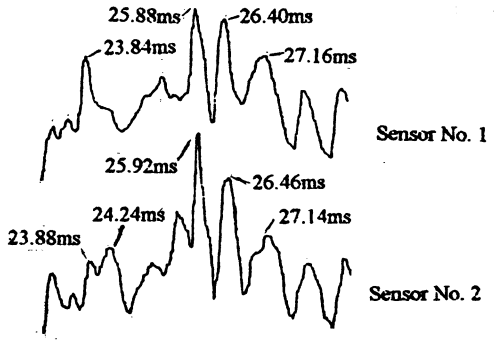

b) Expanded time scale

Figure 8. Dual sensor time traces. $\Delta x + 0.53$mm.

0.53 millimeters. Figure 8b) is an expanded time scale plot of a smaller portion of the traces. Actual times are noted for a number of the points. The largest peaks were found to propagate at $0.4U_e$. The convective speeds of other identifiable points ranged from 0.2 to 0.8 times the freestream velocity.

Space-time correlation measurements for two sensors spaced 2.95 cm apart were made at a distance of 117 cm downstream on the test surface. Figure 9 shows the convective velocities determined from the correlation data. Also shown on figure 9 are three points calculated by Na and Moin (1998) [the points are for the case where the sensor separation distances, $\Delta x \to 0$] for the convective velocity of pressure fluctuations in an adverse pressure gradient that produced separation. The length scale, x/δ_{in}^*, is an arbitrary parameter, which does not directly reflect

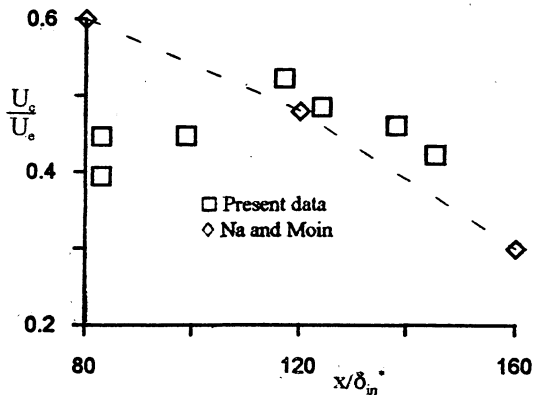

Figure 9. Convective velocities in adverse pressure gradient flows.

the pressure distribution. Figure 9 does demonstrate that the convective velocities are decreased in the adverse pressure gradient flows.

The flow model of an impulse decay-residual viscous layer, Sandborn (1998) employed the convective velocity as the viscous layer characteristic velocity. This model was able to predict the minimum values of the shear stress obtained in the zero pressure gradient flows. The viscous solutions for pressure gradient flows are not readily applied to the time depend case. Solutions, such as Falkner-Skan, would require the flow separate at all times once the pulse decayed to the convective velocity value.

CONCLUSIONS

Experimental evaluation of the time dependent surface shear stress in adverse pressure gradient flows are presented. The large shear pulses previously reported for zero pressure gradient flow are found to persist through to the separation region. The maximum values of the pulses were between 3 to 8 times the mean shear values, and appear to be due to velocity pulses very near the surface of the order of 0.8 times the freestream velocity. The decay of the shear pulse was shown to follow that obtained from impulse flow analysis. The minimum values of the time dependent surface shear stress were between 0.4 and 0.2 times the mean surface shear stress values. Laser velocimeter measurements in the separation region indicate independent positive and negative velocity pulses were present in the wall region.

The statistical characteristic time between the largest shear pulses was evaluated for a range of flow conditions. The times were found to correlate with the mean skin friction

coefficient and a function of the velocity profile Reynolds number and the form factor, which accounted for the pressure gradient.

REFERENCES

Jimenez, J. (1998) LES: Where are we and what can we expect. Paper AIAA-98-2891

Kline, S.J., Reynolds, W.C., Schraub, F.A. and Runstadier, P.W. (1967) Some Preliminary Results of Visual Studies of the Flow Model of the Wall Layers of the Turbulent Boundary Layer. J. Fluid Mech. v.30, pp741

Koskie, J.E. and Tiederman, W.G. (1991) Turbulent Structure and Polymer Drag Reduction in Adverse Pressure Gradient Boundary Layers. Rep. PME-Fm-91-3, Purdue Univ.

Ludwieg, H. and Tillmann, W. (1949) Investigation of the Wall Shearing Stress of Turbulent Boundary Layers NACATM 1284.

Na, Y. and Moin, P. (1998) The Structure of Wall-Pressure Fluctuations in Turbulent Boundary Layers with Adverse Pressure Gradient and Separation. J. Fluid Mech. v. 377, p.347

Orlandi, P. And Jimenez, J. (1994) On the Generation of Turbulent Wall Friction. Phys. Fluids, v.6, pp.634.

Robinson, S.K. (1991) The Kinematics of Turbulent Boundary Layer Structure. NASA TM Sandborn, V.A. (1979) Trends in Turbulent Boundary Layer Engr. Mech. Conf. ASME, U. Of Texas.

Sandborn, V.A. (1998) Surface Shear Stress and Heat Transfer Pulses in Turbulent Boundary Layers. 7th AIAA/ASME Thermophysics and Heat Transfer Conference, Albuquerque, New Mexico.

Schraub, F.A. and Kline, S.J. (1965) Study of the Structure of the Turbulent Boundary Layer With and Without Longitudinal Pressure Gradients. Rept. MD-12, Stanford Univ.

Strickland, J.H. and Simpson, R.L. (1973) The Separating Turbulent Boundary Layer. An Experimental Study of an Airfoil Type Flow. Southern Methodist Univ. Tech. Rept. Wt-2.

Tillman, G, (1994) An Experimental Study of Two-Dimensional Turbulent Boundary Layer Separation. PhD Thesis, Northwestern University.

Watson, E.J. (1955) Boundary Layer Growth. Proc. Roy. Soc. A, v. 231, pp.104.

White, J.B. and Tiederman, W.G. (1990) The Effect of Adverse Pressure Gradient on Turbulent Burst Structure in Low-Reynolds Number Equilibrium Boundary Layers Rept. PME-FM-90-2, Purdue Univ.

Winter, K.G. and Gaudat, L. (1970) Turbulent Boundary-Layer Studies at High Reynolds Numbers at Mach Numbers Between 0.2 and 2.8. Aero. Res. Council, R&M No. 3712.

Nomenclature

A, B, C, D Constants
c_f Skin friction coefficient
c_p Pressure coefficient
F(x) Variation of impulse velocity with x
H Velocity form factor
p Pressure
P(u) Velocity probability
Re/m Reynolds number per meter
R_θ Reynolds number based on momentum thickness
t time
T^+ Non-dimensional time
T^* Non-dimensional time, see figure 4
t^* Time between the large pulses
U_e Velocity at edge of boundary layer
U_i Impulse velocity
U_τ Shear stress velocity
x,y Coordinates
α Impulse velocity exponent
δ_{in}^* Displacement thickness at start of pressure gradient
ϕ Constant
ρ Density
τ_w Surface shear stress
υ Kinematic viscosity

TABLE I. UNCERTAINTIES

Flow properties

Density and viscosity ±1 in the forth figure
Temperature ±0.1 °C
Velocity ±0.05m/s

Reynolds Number Three significant figures

Flow Reynolds number varied by 10% during a set of velocity profile measurements. All velocities were corrected to a mean Reynolds number. Both inlet velocity and temperature varied during extended tunnel operation.

Surface Shear Stress

The surface hot wires were calibrated in a two dimensional channel flow to determine the general voltage-shear stress relation. The calibrations were up dated when mounted in the test flow using velocity profile data and an empirical relation. The up dating accounted for ambient temperature variations.

The surface hot wires were quasi-linearized using a commerical linearizer that allowed an exponent of 5.1. The non-linear calibration errors were reduced to less than 2%.

Frequency response of the sensor-anemometer systems were not measured directly;. The electronic system was limited to approximately 120kHz by the linearizer. Rise times of the order of 50kHz were obtained in high speed flows. The present study employed a digital oscilloscope, that could sample up to 1mHz, to evaluate the individual pulses.

Pulse timing Two significant figures

The present counting techniques were able to measure individual times between pulses accurately to as great as four significant figures. However, statistical averaging of the pulse times were repeatable to only two significant figures.